

PAPER • OPEN ACCESS

A non-Hertzian contact analysis for the ball and raceway of a deep groove ball bearing

To cite this article: Qiang Xi *et al* 2019 *IOP Conf. Ser.: Mater. Sci. Eng.* **542** 012025

View the [article online](#) for updates and enhancements.



IOP | ebooks™

Bringing you innovative digital publishing with leading voices to create your essential collection of books in STEM research.

Start exploring the **collection** - download the first chapter of every title for free.

A non-Hertzian contact analysis for the ball and raceway of a deep groove ball bearing

XI qiang^{1,2*}, PI yangjun^{1,3} and HU yumei^{1,4}

1 Chongqing University, 174 shazheng street, shapingba district, Chongqing, 400044, China

2 cquxiqiang@163.com

3 cqpp@cqu.edu.cn

4 cdrhym@163.com

* The corresponding author

Abstract. Aiming at the premature damage of deep groove ball bearings, considering axial load, elastic-plastic constitutive, coordinated contact and bearing clearance and so on, a non-Hertzian elasto-plastic contact analysis for the bearing ball and the raceway is performed by trans-scale three-dimensional finite element simulation. The results shown that the failure mechanism of the bearing is extremely similar to the L-P fatigue life theory. The effects of load magnitude and direction on contact state were further studied. It indicates that a certain angle of load is beneficial to reduce the maximum internal stress of the bearing, but the angle should not be too large. Besides, increasing the load magnitude results in an increase in the stress value and the depth of maximum stress, but when the load is too heavy, the area that touches the contact surface will be damaged firstly and quickly.

1. Introduction

Gearboxes are widely used in the transmission system of automobiles, and excessive noise and premature breakdowns of the automotive gearboxes are mainly caused by the failure of rolling-element bearings. A typical failure of ball and raceway of a rolling-element bearing in a twin countershaft transmission is presented Fig.1, in which obvious damages are observed.

The failure of transmission bearings is often analyzed by means of fault diagnosis and signal processing. These studies help to identify and distinguish whether the bearings is working properly, but do not fundamentally reveal the mechanism of transmission bearing failure. The origins of failure in rolling bearings are mainly due to the contact of roller and raceway, resulting in such commonly known damages as pitting, spalling, crushing, peeling, scuffing^[1, 2]. Therefore, the study of the real contact situation between roller and raceway is of great importance to the failure prediction of rolling bearings. The contact characteristics between roller and raceway of bearing have been extensively studied by researchers^[3,4,5].

The classical Hertz contact theory is extensively adopted in the counter-conforming contact case. There are two main assumptions in the Hertz contact theory, namely the elastic half-space assumption and the linear elastic constitutive assumption. However, when it comes to the contact problems of roller and raceway as shown in Fig.2, the contact between the ball and inner raceway in the axial symmetrical section, and the contacts between the ball and outer raceway both in the circumferential and axial-symmetrical sections are all conformal contact.



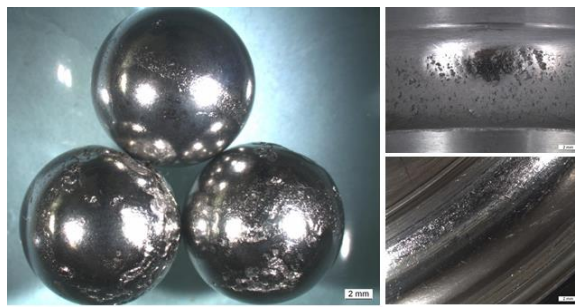


Figure 1. A failure bearing

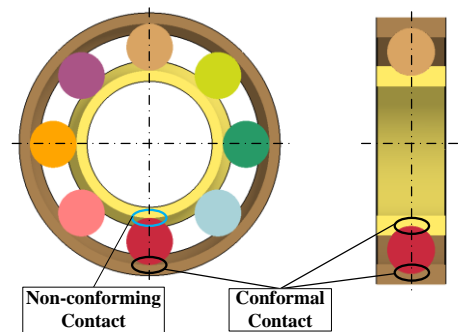


Figure 2. Symmetrical sections of ball bearing

Specifically, in the axial symmetrical section, both inner raceway and outer raceway in contact with ball show a high geometrical adaptation, which no longer meets the Hertzian elastic half-space assumption. Moreover, the real material constitutive model of bearing steel is elasto-plastic^[6]. When the load exceeds the elastic limit and no longer meets the Hertzian linear elastic assumption, it is hard to describe the contact characteristics using elastic constitutive model and the existing theoretical models. It is worthwhile to emphasize that these two non-Hertzian contact factors are significantly important in the contact of ball and raceway of deep groove ball bearings. Goodman and Keer^[7] analyzed the contact of a frictionless sphere in a conforming cavity, they found the contact stiffness in compression deviates more than 25% as predicted by the Hertz theory. Kang et al^[8] also found the contact between balls and raceway of a deep groove ball bearing no longer meets the elastic half-space assumption. They also revised the Hertzian contact equation which determines the relationship of load and deflection proposed by Jones-Harris, and the modified equation is more consistent with the experimental results. Zhupanska^[9] analyzed the problem of normal contact of two identical elastic spheres and equationed the corresponding mixed boundary-value problem at the surface of the sphere, thereby relaxing the assumption of the Hertz theory about small size of the contact area compared to the sizes of the contacting bodies. Comparison of the results with the Hertz theory shows that the latter predicts contact stresses with high accuracy even for relatively large contact areas. The frictional contact problem of a mixed ceramic deep groove ball bearing based on ABAQUS and experiments is analyzed in [10]. The experiments find the maximum contact stress of the ball and raceway exceeds the yield limit, and plastic deformation occurs at the contact area. By comparing the experimental with the simulating results, they find that if nonlinear property of bearing material is not considered, the mutual approach of the ball and raceway would produce large errors.

At present, it is hard to give an accurate theoretical solution considering the conformal contact in the plastic zone to the contact between the ball and raceway of a deep groove ball bearing. An extremely effective means for solving such problem would be FEM. The FEM divides the solution area into a series of units, the denser the unit division, the more accurate the solution. During a two-dimensional contact analysis between the ball and the rigid plate, R L. Jackson^[11] found that when the meshed contact area is controlled to ensure that at least 30 contact elements are always in contact, the maximum contact radius error of 3.3%. However, it is very difficult for three-dimensional contact simulation model to mesh so fine. The trans-scale finite element method enables micron-scale meshing. The main idea of the trans-scale finite element method is perform a coarse mesh finite element analysis first, then extract the contact area for micron-scale modeling, and finally load the node displacement in the coarse mesh model result as a boundary condition into the micron-scale model. The modeling and analysis process of the trans-scale finite element analysis method is described in detail in [12].

In this paper, a non-Hertz contact between the ball and raceway is analyzed by the trans-scale finite element method under actual load boundary conditions. Then, the effect of load magnitude and direction on the contact state is compared. This study will be benefit to the design, wear, lubrication and contact fatigue researches of rolling-element bearings.

2. Method validation

Taking the contact between two hemispheres as an example, the accuracy of the trans-scale simulation method is verified by the three-dimensional Hertz contact theory.

2.1. Obtain theoretical solution

According to the Hertz contact theory, for the two hemisphere contact problems:

Contact radius a :

$$a = \sqrt[3]{\frac{3}{4} \frac{RQ(1-\mu^2)}{E}} \quad (1)$$

Elastic approaching quantity δ :

$$\delta = \sqrt[3]{\frac{9Q^2(1-\mu^2)^2}{2RE^2}} \quad (2)$$

Maximum contact stress P_{max} :

$$P_{max} = \sqrt[3]{\frac{6QE^2}{\pi^3 R^2 (1-\mu^2)^2}} \quad (3)$$

Where R is the radius of the sphere, Q is the compressive load, E and μ is the elastic modulus and Poisson's ratio. The sphere studied here has a spherical radius of 12.5 mm and is made of bearing steel (considering it as an ideal linear elastic material) with a density of 7.85e3Kg/m³, an elastic modulus of 210 GPa and a Poisson's ratio of 0.3. The load of the two hemisphere contact models is set to a radial load of 1000N. The theoretical solution of the contact radius, elastic approaching value and maximum contact stress of the two hemisphere contact model are obtained and shown in table 1.

Table 1. Theoretical solution of two hemisphere contact model

load	contact radius	elastic approaching quantity	maximum contact stress
1000N	0.273mm	23.8μm	6413 MPa

2.2. Obtain numerical solution and comparative analysis

Firstly, a coarse mesh model is solved for the two hemisphere contacts. The spheres were discrete in all hexahedral mesh with an average grid size of about 0.1 mm. The bottom surface of the bottom hemisphere in the three-dimensional contact finite element model is fully constrained, the upper hemisphere constrains all rotation and the translational degrees of freedom in all directions except radial direction (Y-axis). And applies a load of 1000N to the upper surface of the upper hemisphere along the negative direction of the Y-axis. Contact is established between the surfaces of two spheres, regardless of friction, and the coefficient of friction is zero. The material was set to an ideal linear elastic material. The LS-DYNA software is used to solve the coarse mesh model. Based on the simulation results, the micro-scale model meshing area is determined and then solved. The partial model extracted from the coarse mesh model is refined to ensure that the mesh size of the contact area is about 9 μm. So, there are more than 30 units to describe the radius of the contact circle, which can ensure that the number of units participating in the contact is always not less than 30, thereby ensuring the accuracy of the solution.

The results of micro-scale model shows that the maximum contact pressure of the two hemispheres is in the center of the circle, which is about 6067 MPa. The distance between the outer edge nodes of the contact circle is extracted as the diameter of the contact circle. The distance between two nodes that symmetrical about the center of the contact area was measured, and the distance between the two points was 0.562083 mm. That is to say, the contact radius is about 0.281 mm. The comparison between the numerical solution and the theoretical solution of two hemisphere contact is shown in table 2.

Table 2. Comparison between numerical and theoretical solution

	maximum contact stress(MPa)	contact radius (mm)	elastic approaching value(μm)
theoretical solution	6413	0.273	23.8
numerical solution	6067	0.281	25.3
error	5.4%	2.9%	6.3%

It can be seen from table 2 that the error of maximum contact stress, contact radius and elastic approaching value are all within 7%. Therefore, the calculation accuracy of the trans-scale finite element simulation method fully meets general engineering requirements. In addition, according to [12], the trans-scale finite element simulation method has nothing to do with the contact object itself. Therefore, the method can be applied to solve the contact between bearing ball and raceway.

3. 3D non-Hertzian contact of ball and raceway

The analysis of the three-dimensional non-Hertzian contact analysis between the ball and outer raceway is combined with the engineering application and realistic load boundary conditions are considered. Therefore, this paper determines the external load of a bearing and analyzes the load distribution over balls based on a twin countershaft transmission before performing the 3D conformal FEA.

3.1 Calculation of bearing loads

The twin countershaft transmission is quite common in the front-engine front-wheel driving car. The input shaft of the transmission studied here is supported by two deep groove ball bearings on each side, while each of the two countershafts is supported by a deep groove ball bearing on the left side and a cylindrical roller bearing on the right side. The right side of the transmission is close to the engine.

Transmission working at the first and reverse gears, corresponding to the two limit-load conditions of maximum torque, is selected in this analysis. The maximum output torque of the matched engine is 190Nm. Thereby the external loads of the supporting bearings at the operating conditions of first gear and reverse gear are obtained [13]. The result figures out that the maximum loads of deep groove ball bearings appears at the the bearing at the right end of the input shaft, which is consistent with the experimental location of the bearing failure in advance, and the radial force is about 12330N, corresponding to an axial force of about 4678N.

3.2 Load distribution over balls

Load distribution is one of the most important operating characteristics for the ball bearings, and can affect the running accuracy and load carrying capacity. When only the radial external load is considered, Stribeck empirical equation is always used to determine the relationship of the maximum contact force and the radial external load. When the external loads in both radial and axial directions are taken into account simultaneously, the radial and axial integral calculus proposed by Sjövall should be used to get the load distribution over balls. However, the method is quite complex, and it can't consider the influence of clearance which is of critical importance. It should be noted that the assumption of Sjövall

is $\gamma \geq \alpha'$, where $\gamma = \arctan \frac{Fa}{Fr}$ and α' is the contact angle, in which Fa, Fr is the axial and radial external load respectively. When the assumption is not satisfied, the ball bearing will be unstable, and it is hard to analyze the load distribution by theoretical solution. This paper analyzes the load distribution over the balls in a deep groove ball bearing, in which both the axial and radial external loads are taken into consideration, as well as many other factors, such as the clearance, effect of cage-aligning, the gravitational influence of bearing components, are counted in for a more accurate and realistic results. Because of the complexity of the problem, FEA is applied in this paper to determine the load distribution over balls, which produces a more accurate boundary condition for the non-Hertzian contact between ball and outer raceway.

The finite element model (FEM) is established as shown in Fig.3 basing on the structural parameters of the most dangerous bearing, which consists of about 380,000 hexahedral elements.

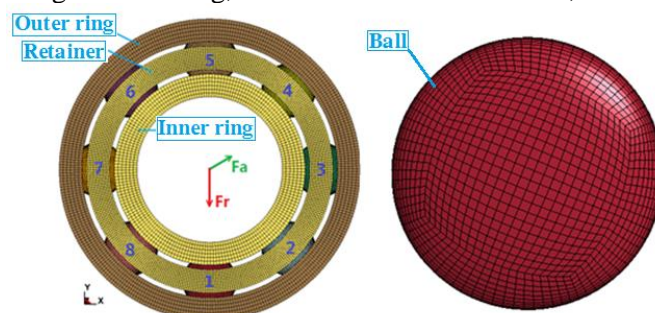


Figure 3. Finite element model of a bearing

As the balls will contact with the retainer and raceway in realistic operating conditions, we make the definition of contacts respectively, totally 24 contact pairs created. Because retainer may contact with the raceway, two more contact pairs are defined. To simulate the interference fit of the outer raceway with the bearing housing, fixed boundary condition is applied to the nodes on the outer surface of the outer raceway. Radial and axial external forces are exerted to the nodes on the inner surface of

the inner raceway, and gravitational acceleration (g) is applied to all the bearing components in the opposite of Y-direction. The material of the balls and raceways are bearing steel, with an elastic modulus of 207Gpa, a density of 7830kg/m³ and a Poisson's ratio of 0.3. The material of the retainer is PA66 nylon, with an elastic modulus of 8.3Gpa, a density of 1145kg/m³ and a Poisson's ratio of 0.28. The load distribution of radial and axial contact forces over the balls are shown in table 3.

Table3. Load distribution of balls (N)

	Ball1	Ball2	Ball3	Ball4	Ball5	Ball6	Ball7	Ball8
Radial	7615.11	4449.48	1018.70	608.62	672.47	608.41	1049.46	4384.27
Axial	385.33	747.85	547.58	532.68	641.45	536.33	555.82	731.83
Total	7624.85	4511.89	1156.54	808.81	929.13	811.06	1187.56	4444.93

It is clear that the maximum total contact force of the bearing occurs at ball 1, with a radial contact force of 7615.11N and an axial contact force of 385.33N. Over the entire load distribution, it exhibits a trend of symmetrical distribution, with the axis of symmetry passing through the sphere centers of ball 1 and ball 5.

3.3 3D non-Hertzian contact

Taking ball 1 as the analysis object, the three-dimensional non-Hertzian contact analysis of the ball and the outer raceway is carried out according to the trans-scale simulation method in literature [12]. The simulation results obtained from the previous ball load distribution analysis are used as the results of the coarse mesh model, and the determined micro-scale model meshing area is judged accordingly. As shown in Fig.4, the inside of the white frame is the micro-sized model meshing area.

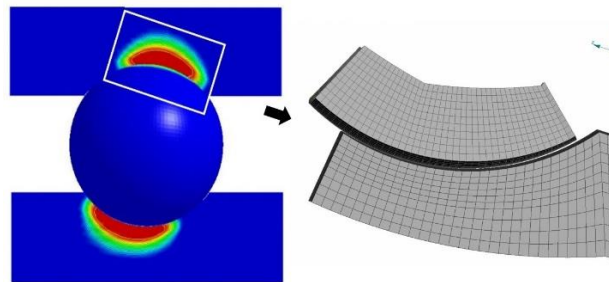


Figure 4. Micro-sized model meshing area of ball and raceway contact

The micro-scale model is then solved. The partial model extracted from the coarse mesh model is refined to ensure that the mesh size of the contact area is about 20 μm . So, the ratio of the short half axis of the contact ellipse to the unit size is about 18, which can ensure that the number of units participating in contact is always more than 30, thereby ensuring the accuracy of the solution. The load of the micro-size model is consistent with the coarse model. All degrees of freedom on the outer surface of the outer raceway are constrained. Contact is established between the ball and outer raceway, and the dynamic and static friction coefficients are both set to 0.002. This paper selects an elasto-plastic constitutive model for the material of the ball and raceway, with MAT024-PIECEWISE-LINEAR-PLASTICITY in the commercial finite element software LS-DYNA to describe. Since the contact analysis of ball and raceway under radial and axial loads belongs to quasi-static analysis, it is unnecessary to consider the effect of strain rate on the plasticity of the material. In addition, a static compression experiment of the bearing material is carried out, and the true stress-strain curve of the material is obtained, and then loads into the model. The yield strength of the material is about 1684Mpa.

4. Results and discussion

4.1. Results

First, as shown in Fig.5 and Fig.6, the contact pressure distribution on the contact surface between the ball and raceway is substantially elliptical (not completely elliptical for axial force existing). And the contact pressure on surface is gradually increased from the outside to the inside, and the maximum value appears at the center of the contact area. The maximum contact pressure on surface of the ball is about 2984 MPa, and the maximum contact pressure on raceway surface is about 2759 MPa.

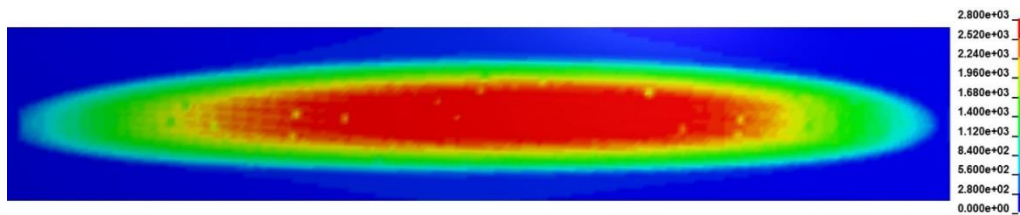


Figure 5. Contact pressure distribution of the contact surface of ball

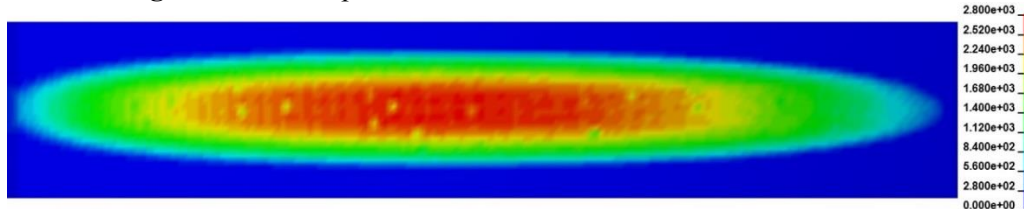


Figure 6. Contact pressure distribution of the contact surface of raceway

In addition, the premature damage of bearing is also closely related to the V-M stress distribution of the contact area. In order to obtain the V-M stress distribution of the contact area, the micro-size model is cut along the axial and circumferential symmetrical middle planes of the bearing. The V-M stress distribution in the cutting plane of the micro-scale model is shown in Fig.7 and Fig.8.

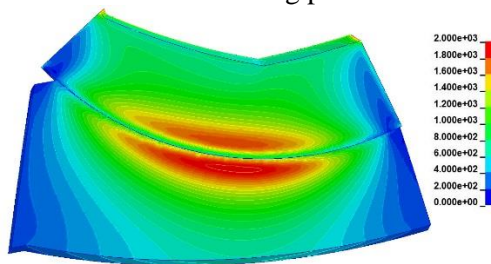


Figure 7. Axial sectional view

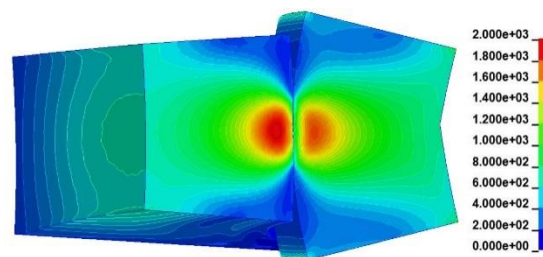


Figure 8. Circumferential sectional view

It can be clearly shown from the two cross-sectional views that the distribution of effective stress distribution in the axial symmetrical section with higher geometrical adaptation is also significantly different from the circumferential symmetrical section with lower geometrical adaptation. The V-M stress distribution is semi-elliptical in the circumferential symmetrical section, and is quite similar with the 2D Hertzian results. However, within the axial symmetrical section, with higher geometrical adaptation, the effective stress distribution forms an elongated strip, distinguishing from the Hertzian distribution. Besides, the maximum V-M stress does not appear on the contact surface, but below the contact surface.

In addition, the simulation results show that the maximum V-M stress of the ball and the raceway is about 1752 MPa and 1968 MPa. However, the yield strength of the bearing material is 1684 MPa. That is to say, the V-M stress of the bearing analyzed in this paper exceeds the yield strength of the material under the limit load condition. Therefore, we extract the variation curve of the maximum contact pressure, maximum equivalent stress and maximum shear stress of the ball and the outer raceway during the contact process as Fig.9 shown.

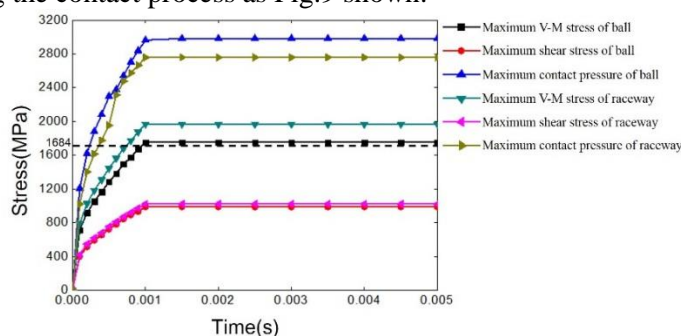


Figure 9. Contact characteristics change process

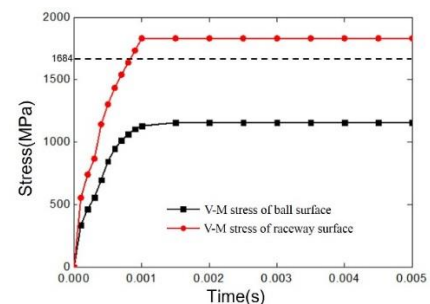


Figure 10. Maximum V-M stress on surface

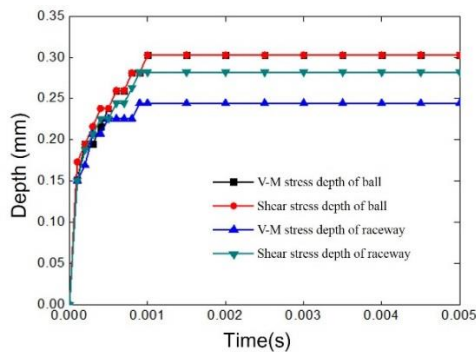


Figure 11. Stress depth change process

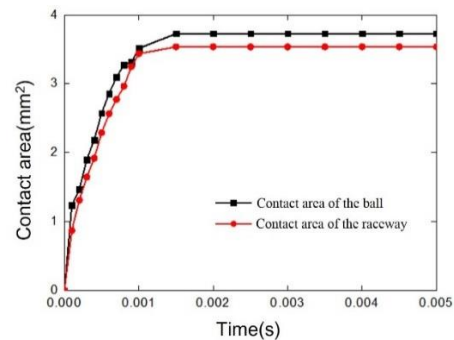


Figure 12. Contact area change process

It can be seen from the figure that the maximum shear stress values of the balls and the outer raceway are not much different at each moment, and the former is always slightly smaller than the latter. When the load is stabilized, the maximum shear stress of the ball and the outer raceway is stable at about 1000 MPa. However, the bearing steel is a plastic material with a tensile strength of about 1600 MPa. The shear stress limit is generally considered to be 0.5 to 0.7 times the tensile strength, that is, 800 to 1120 MPa. That is to say, both ball and raceway are highly likely to be damaged. The maximum V-M stress of the ball slightly exceeds the yield strength of the material at the time of loading, and finally stabilizes at about 1752 MPa, exceeding the yield strength of the material by 4%; The maximum V-M stress of the outer raceway reached the yield strength of the material at the time of loading too, and finally stabilized at around 1968 MPa, exceeding the yield strength of the material by 17%. The maximum contact pressure of the ball and the outer raceway are both quickly exceed the yield limit of the material, but the V-M stress of the ball contact surface ball never reaches the material yield limit, and is stable at about 1157 MPa; The V-M stress value of the outer raceway contact surface has reached the yield limit and is stable at about 1832 MPa. The stress variation curve of the unit with the largest V-M stress on the contact surface is shown in Fig.10. The maximum V-M stress depth, the maximum shear stress depth and the contact area of the ball and the outer raceway are shown in Fig.11 and Fig.12.

It can be seen that, as the load increases, the maximum V-M stress and the maximum shear stress depth of the ball gradually increase, and finally reach stability after loading is completed, and the stable value is 0.303 mm; The maximum V-M stress and the maximum shear stress depth of the outer raceway is also gradually increasing, the final stability is 0.245mm and 0.282mm. Besides, the contact area of the ball is always slightly larger than the outer raceway, and the stress depth of the ball is always greater than the outer raceway. Therefore, the bearing volume of the ball will always be larger than the outer raceway, which is an important reason why the V-M stress of the outer raceway is higher than the ball. In addition, the maximum shear stress and the maximum V-M stress of the ball appear at the same depth at each moment. However, the maximum shear stress depth of the outer raceway begins to exceed the maximum equivalent stress depth when the load is loaded halfway.

In summary, the bearing volume of the ball is larger than outer raceway, the maximum V-M stress value of the ball is smaller than outer raceway, and the maximum shear stress value of the ball is slightly smaller than outer raceway. Therefore, the bearing analyzed in this paper will yield at the subsurface of outer raceway first. Meanwhile, the V-M stress on the outer raceway surface exceeds the yield strength of the material too. So, both the surface and the subsurface of outer raceway will initiate cracks. Subsequently, for the continuously rolling effect of the ball and raceway, crack that initiated at the subsurface of raceway extends to the surface, and connects with the crack initiated at the surface. As we can see in Fig.1, the inner raceway and the ball are also damaged. The reason is that parts of the lubricating oil immerses into these cracks. Under the hydrodynamic pressure and alternating loads of bearing operating, parts of the material are removed from the original base of ball and raceway, which results in pitting and spalling. Furthermore, these removed materials will act as abrasives, with the bearing operating, piercing the film and scratching the ball and raceway, which significantly reduce the lubricating properties of the grease. Meanwhile, due to the large pieces of peeling, the running accuracy of the bearing decreases, and additional impact is generated, which accelerates bearing failure.

Obviously, the damage mechanism of the bearing analyzed in this paper is very close to the fatigue life theory of Lundberg and Palmgren ^[14]. According to the subsurface initiated crack mechanism, the crack will first occur at the core of maximum shear stress under alternating loading, and gradually extends to the surface, and connects with the surface initiated pitting, which results in pitting and spalling. Besides, the survival probability of the load carrying volume is determined jointly by the stress cycles, Weibull life distribution, the peak of the maximum shear stress and the contact depth of the peak maximum shear stress, whereas the load carrying volume is related to the sizes of the contact area.

4.2 Further discussion

The magnitude and direction of the load have a significant impact on the static contact state of the ball and raceway. Therefore, this paper analyzes the effect of load magnitude and direction on the non-Hertzian contact of bearing ball and raceway. The load vector in the previous article has an angle of about 2.9 with the radial direction of the ball. Keep the load size constant, set the load angle to 0, 2.9°, 5°, 10°, 15°, 20°, and extract the maximum equivalent stress, maximum shear stress and stress depth of the outer race as Fig.13 and Fig.14 shows.

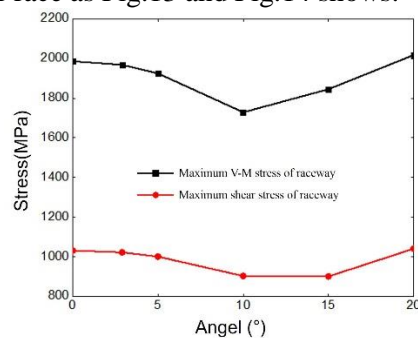


Figure 13. Effect on maximum stress

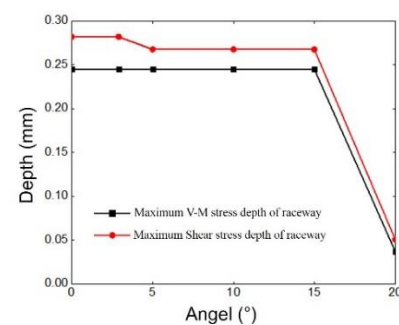


Figure 14. Effect on the maximum stress depth

It can be seen that, as the angle increases, the maximum V-M stress and the maximum shear stress decrease first and then increase. It reaches the minimum when the angle is 10°, and decreases by 7.1% and 6.9% compare to the value while the angle is 0°. The maximum V-M stress and the maximum shear stress depth do not change much as the angle increases, but suddenly decrease when the angle reaches 20°. It indicates that the deep groove ball bearing can withstand a certain degree of axial load, and a certain angle of load is beneficial to reduce the maximum stress value of the bearing, but the angle should not be too large. The reason might be that, due to the geometric coordination, the load with a certain angle can make the load on the ball more transmitted to the raceway through the periphery of the contact area instead of being excessively concentrated in the contact center, thereby reducing the stress value. When the angle exceeds a certain limit, the contact center is excessively deviated due to the excessive declination, so that the contact area is likely to reach the shoulder of the raceway, which resulting in a decrease in the bearing volume, thereby resulting in an increase in the stress value.

Then, keep the angle constant and solve the model with radial loads of 5000N, 7615.11N, 10000N, 15000N, 20000N. The changes in maximum V-M stress, maximum shear stress, and stress depth are shown in Fig.15 and Fig.16.

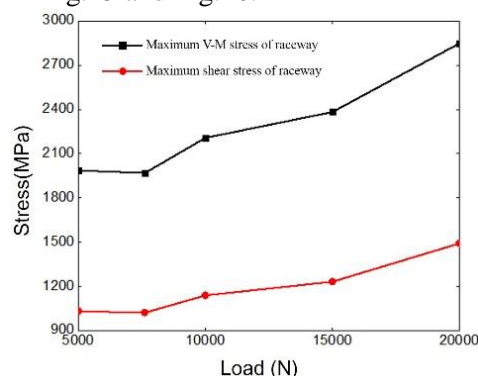


Figure 15. Effect on maximum stress

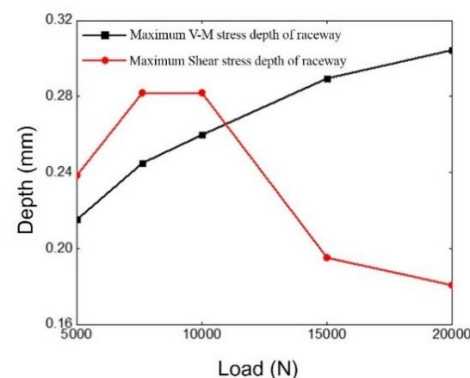


Figure 16. Effect on maximum stress depth

It can be seen that, as the load increases, the maximum V-M stress, the maximum shear stress, and the maximum V-M stress depth increase gradually, the maximum shear stress depth increases first, then flattens, and finally decreases. This indicates that increasing the load value results in an increase in the stress value and yield depth. However, when the load is too heavy, the area that touches the contact surface will be damaged firstly and quickly. The drop in the maximum shear stress depth in Fig.16 maybe due to this.

5. Conclusion

This paper analyzed the contact between ball and raceway of a deep groove ball bearing of a two-shaft transmission by trans-scale finite element method. The non-Hertzian contact between the ball and outer raceway under extreme working conditions is obtained. Based on this, the bearing damage mechanism and process is analyzed. The result indicates that the damage mechanism of the bearing is very similar to the failure mechanism predicted by L-P fatigue life theory.

This paper analyzes the effect of load magnitude and direction on the non-Hertzian contact of bearing ball and raceway. The result shows that a certain angle (about 10) of load is beneficial to reduce the maximum internal stress of the bearing, but the angle should not be too large. Besides, increasing the load magnitude results in an increase in the stress value and the depth of maximum stress, but when the load is too heavy, the area that touches the contact surface will be damaged firstly and quickly.

6. References

- [1] M Littmann, W. E. The mechanism of contact fatigue. Interdisciplinary approach to the lubrication of concentrated contacts, (Ed. P. M. Ku) Proceedings of a Symposium, Troy, NY, July 1969; NASA Special Report, SP-237, 1970; PP. 309-378(NASA, Washington DC).
- [2] Olver AV, The mechanism of rolling contact fatigue: an update, Proceedings of the Institution of Mechanical Engineers, Part J: Journal of Engineering Tribology. 2005; 219:313-30.
- [3] Srečko Glodež, Rok Potočnik, Jože Flašker. Computational model for calculation of static capacity and lifetime of large slewing bearing's raceway. Mechanism and Machine Theory. 2012; 47:16-30.
- [4] Albert V.Korolev, Andrey A.Korolev, Radoslav Kreheř. Character of distribution of the load between the balls in the ball bearings under the action combined of external load. Mechanism and Machine Theory. 2014; 81:54-61.
- [5] El-Thalji I, Jantunen E. A descriptive model of wear evolution in rolling bearings. Engineering Failure Analysis. 2014; 45:204-224.
- [6] Linares Arregui I, Alfredsson B. Elastic-plastic characterization of a high strength bainitic roller bearing steel-experiments and modeling. International Journal of Mechanical Sciences. 2010; 52:1254-1268.
- [7] L.E.Goodman, L.M.Keer. The contact stress problem for an elastic sphere indenting an elastic cavity. International Journal of Solids and Structures. 1965; 407-415.
- [8] Kang Y, Shen PC, et al. A modification of the Jones-Harris method for deep-groove ball bearings. Tribology. 2006; 39:1413-1420.
- [9] Zhupanska OI. Contact problem for elastic spheres: Applicability of the Hertz theory to non-small contact areas. International Journal of Engineering Science. 2011; 49:576-588.
- [10] Xu Q, Ren CZ, Chen JJ. Three dimension FEM analysis of interface and contact stress of hybrid ceramic ball bearing. Machine tool & Hydraulics. 2003; No2:203-204,206.
- [11] Robert L.Jackson, Itzhak Green. A Finite Element Study of Elasto-Plastic Hemispherical Contact Against a Rigid Flat [J]. ASME .Journal of Tribology.2005, 127(2):343-354.
- [12] Xie Hao. Research on Local Model-Based Contact Simulation of Ball Bearings [D]. Chongqing University, 2016.
- [13] Lan Jiangming. A non-Hertzian contact analysis for the ball and raceway of a transmission bearing [D]. Chongqing University, 2015.
- [14] G. Lundberg, A. Palmgren. Dynamic capacity of rolling bearings. Acta Polytechnica Mechanical Engineering Sciences. 7(3):1-7, 1947.